# Aerodynamics of a Finite Aspect Ratio Jet Flap at Low Flight Speeds

F. L. Addessio*
*Rocketdyne Division of Rockwell International Corporation, Canoga Park, Calif.*
and
J. G. Skifstad†
*Purdue University, W. Lafayette, Ind.*

**A theory is presented for inviscid incompressible flow past a thin wing equipped with a part-span jet flap, and is capable of treating low-speed flight regimes where the induced aerodynamic field of the jet is not small. The nonlinear problem is handled by treating the induced flowfields of the jet and the wing separately, obtaining the fully coupled solution in an iterative manner. A lifting surface theory is employed for the aerodynamics of the wing. The vorticity associated with the jet is assumed to lie on the locus of the jet, which is obtained in the solution. Spanwise variation of the jet vortex strength is assumed to be elliptical in the analysis. The theory is considered to be better able to evaluate subsidiary aerodynamic variables, such as the downwash in regions aft of the wing, as well as forces and moments on the wing, than comparable linear or nonlinear theories. Computational results are presented for the force system on a rectangular wing, comparing them with existing linear theories and experimental data. Good agreement is found for small angles of attack, jet deflection angles, and jet momentum coefficients where the linear theories and experimental data are applicable. Results also are presented for larger values of the previous parameters where the linear theories are not suitable. Downwash data at a point in the vicinity of a control surface, the load distribution on the wing and the jet, and the jet location also are presented for representative flight conditions.**

## Nomenclature

$a_i$ = constant employed in the expansion for the jet location
$C_D$ = drag coefficient
$C_J$ = jet momentum coefficient
$C_n$ = constant coefficients employed in the expansion for the jet vortex strength
$C_L$ = lift coefficient
$C_P$ = pressure coefficient
$c$ = chord
$E,K$ = first and second complete elliptic integrals
$\boldsymbol{e}$ = unit vector
$e$ = numerical damping factor
$f$ = functional representation for the vortex sheets, $z=f(x,y)$, $f_J$ for the jet and $f_A$ for the airfoil; arbitrary function
$G,g$ = streamwise distribution of the jet vortex strength
$H$ = spanwise distribution of the jet vortex strength
$J$ = jet momentum flux per unit span
$k,k_c$ = modulus and complimentary modulus of the elliptic integrals
$M$ = number of terms in the expansion for $f_J$
$\boldsymbol{n}$ = unit vector normal to the jet sheet
$n$ = index
$N$ = number of terms in the expansion for $dg/dx$
$\boldsymbol{R},R$ = distance from a source point to a field point and its magnitude
$S$ = surface area
$s$ = span
$U_\infty$ = freestream velocity
$\boldsymbol{V}$ = total velocity vector with components $(U,V,W)$
$\boldsymbol{v}$ = disturbance velocity vector with components $(u,v,w)$
$\boldsymbol{x}$ = position vector $(x,y,z)$
$x,y,z$ = rectangular coordinates
$x^*$ = $\nu x/s_J$
$X$ = $x$ position chosen to separate the near field domain from the far field
$\alpha$ = angle of attack
$\beta,\nu$ = scaling factors
$\boldsymbol{\gamma}$ = vortex strength vector
$\Gamma$ = circulation
$\rho$ = mass density of air
$\theta$ = downwash angle; angle in Eq. (15)
$\kappa$ = jet curvature
$\xi,\eta,\zeta$ = curvilinear coordinates associated with the jet sheet
$\tau$ = deflection angle of the jet

*Subscripts*

$J$ = jet
$A$ = airfoil

Received Oct. 27, 1976; revision received May 13, 1977.
Index category: Aerodynamics.

*Technical Staff; formerly Research Assistant, School of Mechanical Engineering, Purdue University.

†Professor, School of Mechanical Engineering. Member AIAA.

## Introduction

A JET flap, illustrated in Fig. 1, contributes to the lift of a wing in two ways: 1) the aerodynamic field is altered by the jet, increasing the net lifting pressure force on the surface of the wing; and 2) the reaction to the momentum flux of the jet contributes to the lift. The jet flap is one of several powered-lift concepts of interest in STOL aircraft design. It is perhaps the simplest and of limited practical interest, but the aerodynamics problems associated with the jet flap are common to most powered-lift schemes. Analyses of the more elementary jet flap problem offer one approach for examining the characteristics of this class of problems in a manageable context.

One of the first analytic investigations of the jet flap scheme was a two-dimensional theory developed by Spence.[1] This was later extended to handle the three-dimensional problem with limitation to elliptic loadings, constant jet momentum coefficients, and constant jet deflection angles.[2] Several theories seeking to provide more generality have been

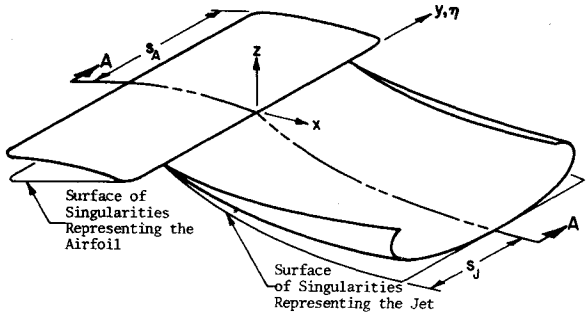


a) Locations of the Singularities and the Stream Surfaces

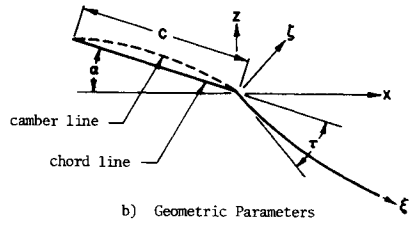


b) Geometric Parameters

**Fig. 1 Jet flap and airfoil geometry.**

published. Those of Kerney[3] and Tokuda[4] employed matched asymptotic expansions to yield methods capable of handling more general wing-flap configurations. The lifting surface theory of Lopez and Shen[5] and Shen, Lopez, and Wasson[6] offered the further advantage of treating augmentor wings and blown flaps. Other theories considering the ground effects problem[7] or providing more rapid computation techniques[8] now are available. All of these methods employ approximations inherent in linear theories; that is, all flow angles are assumed to be small. It may be expected that such theories should be capable of providing good results for the forces and moments on the wing, at least for situations in which the jet flap is at a small angle to the freestream, or where the momentum flux is small. The accuracy of these methods for the purpose of computing the downwash field, or where the jet plays a more dominant role in the aerodynamics, remains open to question. In the past few years, two-dimensional theories have been reported[9,10] which account for nonlinearities, considering the more general problem.

Each of the existing theories may account adequately for parts of the overall problem, but none may be expected to be capable of treating the entire spectrum of flight regimes and jet loadings. With low jet loadings and sufficient airspeed, for example, the field induced by the jet may be regarded properly as a small perturbation to the basic aerodynamic field. With higher jet loadings and lower airspeeds, this may not be acceptable. If computation of the downwash field near airframe members such as the tail surface is to be required, along with forces and moments on the wing, additional care in the treatment of the jet is required. Also, there are regimes of flight demanding yet other factors, such as consideration of the ground plane, be included in the theory.

The analysis described herein is intended to include the situation in which the induced aerodynamic field of the jet is not small by comparison with the normal aerodynamic field of the vehicle. It applies to wings with jet flaps of either high or low loadings and offers the additional benefit of improved downwash computations. The essential influences of the finite aspect ratios of the wing and the jet are included in the theory.

## Formulation of the Analytical Model

The low-speed aerodynamics problem considered in the analysis is that of a symmetric wing with a symmetric full- or part-span jet flap. Compressibility and viscous effects are ignored in both the aerodynamic field and the jet.

A wing with a thin jet exhausting from its trailing edge exhibits a flowfield illustrated schematically in Fig. 1 (bold outlines identify stream surfaces). Both the wing and jet are shown as single surfaces: the wing as a cambered sheet of zero thickness in the tradition of thin wing theory,[11] and the jet as a jet sheet[1] of infinitesimal thickness. These are approximations common to most analyses, including that to be considered here. The finite thickness of the wing, the viscous growth of the jet, and its entrainment may be treated without major modification of the theory, but they complicate the discussion and are not dominate factors in the problem.

Referring to Fig. 1, the problem requires determination of the distribution of bound vorticity on the wing and the jet sheet, that of free vortices shed by either (not shown in Fig. 1), and the geometry of the jet sheet. If the jet exhausts at a large angle to the freestream flow, and if $C_J$, the jet momentum coefficient, is high, it must be considered inappropriate in any reasonable approximation to assume the vorticity of the jet positioned in a plane behind the wing, parallel to the freestream. Rather, the position of this vorticity should be associated closely with the jet sheet. This is particularly true if the theory is expected to provide results for the downwash field behind the wing, as well as the wing loading.

The geometry of the jet sheet may be expected to be quite complex, giving rise to mathematical complications, which are both prohibitive and unnecessary if the theory is not required to represent well the details of the flow in the immediate vicinity of the jet. Two observations may be made which enable substantial simplification of the problem. First, the region of the jet most important in this problem is that within a few chord lengths of the airfoil. The lateral vorticity component decreases with distance from the wing, and the field far from the wing may be approximated suitably by a plane vortex sheet. Second, in the near-field region, the momentum of the jet renders it relatively "stiff," making effects such as rollup of the vorticity of minor importance there.‡

Taking these observations into account, the geometry of the theoretical model may be simplified in the following manner. The one aspect of the geometry of the jet sheet (and its vorticity distribution) considered of principal importance here is its location, as described by a curve in the plane of symmetry of the problem. The part of that trajectory which should be best represented is that within a few chord lengths of the wing. Since rollup is to be neglected, some approximation must be made as to the lateral geometry (cross section) of the jet sheet. Now, rather than specifying some functional form for the lateral cross-sectional contour of the jet sheet, it is useful to specify a functional form for the lateral distribution of vorticity and to let the cross-sectional contour of the jet sheet take whatever form it may. This substantially simplifies the theory, and is no more objectionable than assuming a lateral contour for the jet sheet.

The theoretical model employs an elliptic distribution for the lateral component of vorticity on the jet.§ The vorticity associated with the jet sheet is assumed to lie on a surface generated by straight lines parallel to the trailing edge of the airfoil and passing through the locus of the jet sheet in the plane of symmetry. The jet sheet coincides with this surface containing the vorticity only at the plane of symmetry, but should not depart greatly from that surface. The geometry is illustrated in Fig. 1.

The bound vorticity of the wing was assumed to lie in the $z = 0$ plane. The vorticity on the sheet behind the wing

‡It should be kept in mind that these remarks apply to the conditions discussed for this analysis and are not necessarily appropriate for more general conditions.

§This is a mathematical convenience, plausible but hardly precise. Others have employed elliptic distributions.[2] The information sought here requires integrals over the distribution, reducing the need for precision in the form of the distribution.

(physically, the jet sheet) is regarded as the sum of two contributions; that associated with the vorticity shed by the wing surface and a dominant part, which is associated with the jet. The latter, of primary concern here, is located on the jet sheet in the computational scheme, whereas the former is approximated in the mathematics as lying in the plane of the wing. Locating the shed vorticity contribution associated with the wing in a plane behind the wing surface for computational purposes enabled substantial simplification of the analysis, and was not found to compromise the results materially for the cases of interest. The flowfield arising as a result of all of the vorticity, the sum of that associated with the wing and that associated with the jet, is required in the solution to meet appropriate boundary conditions on the jet sheet and the wing surface.

A solution for this problem may be obtained as follows. 1) A flowfield for the wing alone is employed as a first approximation to account for the influence of the wing on the jet. This may be as simple as a lifting line approximation, or a more detailed solution, if readily available. 2) A solution for the jet is obtained subject to the influence of the combined fields of the wing and the freestream. This solution yields both the distribution of the bound vortex strength along the jet and the position of the jet sheet. 3) The combined jet solution and freestream flow then are taken as a new imposed field for a detailed solution of the wing problem. The solution procedure employed for that purpose is of the lifting surface type.[11] Given these results, the forces and moments on the wing may be obtained by direct integration, and the velocity field at points of interest in the vicinity of the wing or jet may be computed as needed. The last airfoil solution may be employed as a new initial condition, repeating the entire procedure until acceptable solutions are obtained.

The analysis of the jet subject to the influence of the freestream and the disturbance field of the wing is referred to here as the jet problem. That of determining the aerodynamic field of the wing subject to the freestream and the field of the jet is termed the airfoil problem.

## General Relations

The coordinate system employed in the analysis, along with the principal geometric parameters, are illustrated in Fig. 1. For some purposes in the jet analysis, it is convenient to employ an orthogonal curvilinear coordinate system within the jet sheet: $\xi$ in a streamwise direction, $\eta$ in the spanwise direction, and $\zeta$ normal to the sheet. Referring to Fig. 1, the two principal angles are defined in the cross-sectional view. The angle of attack $\alpha$ is the angle measured from the $x$ axis to the chord line and the jet deflection angle $\tau$ from the chord line to a line, which is tangent to the jet as it leaves the trailing edge of the airfoil. The notation pertinent to the span lengths and the airfoil chord are also shown in the figure.

The relations required in the theory may be obtained from the Helmholtz Theorem.[12] Employing the concept of a vortex sheet, the disturbance velocity field ($v$) may be related to the vortex strength of the sheet ($\gamma$) by the relation

$$v(x)=\frac{1}{4\pi}\int\int_S \frac{\gamma' x R}{R^3}\,dS' \tag{1}$$

where $S$ represents the totality of vortex sheets, and

$$R=|R|=[(x-x')^2+(y-y')^2+(z-z')^2]^{1/2}$$

$$v=V-U_\infty e_x$$

In the previous equations, integration is with respect to the source coordinates ($x'$), the disturbance velocity is a function of the field point ($x$), and $V$ is the total velocity vector.

The requirements that the surfaces of the wing and the jet be stream-surfaces (the kinematic conditions) yield

$$V\cdot\nabla[f(x,y)-z]=0 \tag{2}$$

where $z=f(x,y)$ is an equation for the appropriate surface (denoted $f_J$ for the jet and $f_W$ for the wing).

Now, the location of the jet is not known initially. An additional condition must be applied to the jet sheet accounting for the momentum change of the jet due to normal pressure forces acting on it. For a jet thin compared to its radius of curvature ($1/\kappa$), this additional condition (the dynamical condition) may be written

$$\kappa=\frac{2(\gamma\times n)\cdot V_m}{C_J U_\infty^2 c} \tag{3}$$

where

$$V_m=(V^+ + V^-)/2$$

is the mean velocity at a point located on the jet sheet and $C_J$ is the jet momentum coefficient:

$$C_J=2J/\rho U_\infty^2 c$$

The curvature in the $y=0$ plane, $\kappa$, may be expressed in terms of $f_J(x,0)$ as follows:

$$\kappa=|f_J''|/(1+f_J'^2)^{3/2} \tag{4}$$

Equation (3) is to be satisfied in the analysis only at points on the jet sheet in the plane of symmetry where the jet sheet coincides with the sheet of singularities representing the jet vorticity. This condition is not met strictly at any other points on the jet sheet, of course, within the approximations involved in the analysis.

## Solution of the Jet Problem

The jet problem requires determining the vortex strength distribution and the location of the jet sheet subject to the influence of both the freestream and the disturbance field created by the wing. The field induced by the wing is assumed to be known in this computation. Equations (2) and (3) must be satisfied at points on the surface in the plane of symmetry, with $v$ given by Eq. (1).

By definition, the vortex strength vector ($\gamma$) lies within the vortex sheet. Recalling the curvilinear coordinate system ($\xi,\eta$) located on the jet sheet, the vortex distribution associated with the jet may be expressed as

$$\gamma_J(\xi,\eta)=\gamma_{J\xi}e_\xi+\gamma_{J\eta}e_\eta \tag{5}$$

The assumption that the distribution of the spanwise component of the vortex strength of the jet has the same functional form at all streamwise positions along the jet implies that the components of the vortex strength may be written

$$\gamma_{J\xi}=G(\xi)H(\eta) \tag{6}$$

and, from the solenoidal property of $\gamma$,

$$\gamma_{J\eta}=-dG/d\xi\int_{-s_J}^{\eta}H(\eta')\,d\eta' \tag{7}$$

For the elliptic distribution considered,

$$\int_{-s_J}^{\eta}H(\eta')\,d\eta'=[1-(\eta/s_J)^2]^{1/2} \tag{8}$$

The unknown functions $f_J$ and $G$ were represented in the analysis by truncated series with coefficients to be determined in the solution. The semi-infinite domain, $0<x<\infty$, was divided into two regions, a near field, $0<x<X$, and a far field extending beyond $X$. The functional representations in the near field were of primary concern. Those in the far field were chosen to facilitate integration in that domain; that choice is not critical in the solution since contributions to the integrals from that region are small if $X$ is large enough (5-10 chord lengths).

The lateral component of vorticity $\gamma_{Jy}$ decreases monotonically with increasing $x$; it must ultimately approach zero. Moreover, the function of $dg/dx$, where $g(x) = G[\xi(x,f_J)]$, should display a logarithmic singularity at the origin as suggested by the two-dimensional theory of Spence.[2] Consequently, the series expansion for $dg/dx$ was taken to be

$$dg/dx = -\sum_{n=1}^{N-1} C_n\, n \exp\left(-\frac{n\beta x}{s_J}\right) + C_N \ell n\left(\frac{x}{s_J}\right)\Big/\left(\frac{x}{s_J}+1\right)^{3/2} \tag{9}$$

The factor $\beta$ is a scaling parameter, chosen to best represent the functions encountered over the near-field domain. This functional representation was applied to the entire semi-infinite domain.

The series representing $f_J$ in the near field ($x<X$) was chosen to have the form

$$f_J = -x\tan(\tau+\alpha) + \frac{s_J}{\nu}\sum_{i=1}^{M} a_i\left[ix^* - 1 + \frac{1}{(x^*+1)^i}\right] \tag{10}$$

where $x^* = \nu x/s_J$ and $\nu$ is a suitable scale factor. The jet was assumed to have a constant slope in the far-field region, equal to the slope at $x=X$. This representation was not precise, of course, but simplified the integrals considerably and should not seriously detract from the merit of the solution. Considering an inviscid problem, where the sheet would be allowed to roll up, the resulting trailing vortex pair would have a constant slope, apart from viscous interactions.

Given the previous functional forms for $g$, $H$, and $f_J$, the resulting equations for the disturbance velocities, from Eqs. (1), become

$$u(x,0,f_J) = u_A(x,0,f_J) - \frac{1}{2\pi s_J^2}\sum C_n \int_0^\infty \left[g_n \frac{df_J}{dx'} k_J (K-E) + \frac{dg_n}{dx'}(z-f_J)\frac{k_J}{k_{cJ}^2}(E-k_{cJ}^2 K)\right] dx' \tag{11}$$

and

$$w(x,0,f_J) = w_A(x,0,f_J) + \frac{1}{2\pi s_J^2}\sum C_n \int_0^\infty \left[g_n k_J (K-E) + \frac{dg_n}{dx'}(x-x')\frac{k_J}{k_{cJ}^2}(E-k_{cJ}^2 K)\right] dx' \tag{12}$$

where $u_A$ and $w_A$ are the components of the disturbance field created by the wing and $g_n$ ($dg_n/dx'$) denote the coefficients of $C_n$ in the series expansion for $g$ ($dg/dx$): refer to Eq. (9). The functions $g$, $dg/dx'$, $f_J$, and $df_J/dx'$ are regarded as functions of $x'$ in Eqs. (11) and (12). The functions $K$ and $E$ are complete elliptic integrals of the first and second kinds, respectively, with modulus

$$k_J = s_J^2/[s_J^2 + (x-x')^2 + (z-f_J)^2] \tag{13}$$

The kinematic and dynamic conditions in the plane of symmetry ($y=0$ plane) of the jet sheet may be expressed in the forms

$$U_\infty + u(x,0,f_J)(df_J/dx) - w(x,0,f_J) = 0 \tag{14}$$

$$\kappa = \frac{2\gamma_{Jy}\{[U_\infty + u(x,0,f_J)]\cos\theta - w(x,0,f_J)\sin\theta\}}{C_J U_\infty^2 c} \tag{15}$$

where

$$\sec\theta = [1 + (df_J/dx)^2]^{1/2} \tag{16}$$

recalling that $f_J(x,y) - z$ describes the jet surface.

Equations (14) and (15), with $u, w$, and $\kappa$ provided by Eqs. (4, 11, and 12), comprise a pair of algebraic equations for the $M+N$ unknown coefficients ($C_n$ and $a_i$). With a finite number of terms ($M+N$) it is not possible, of course, to satisfy these equations at all points in the semi-infinite domain. The equations can be satisifed exactly only at $(M+N)/2$ points at most. It is advisable, however, to satisfy the relations in a broader sense over the domain. This was accomplished by requiring the equations to be solved in a least-squares sense over the entire near-field domain.[13]

### Numerical Aspects of the Jet Problem

The numerical procedure employed to obtain the solution to the previous system of equations was an iterative one. A set of control points was chosen spanning the near-field domain $0<x<X$. The number of points was chosen to be several times the value $(M+N)/2$ such that a least-squares method would yield smooth functions $f_J$ and $g$, and so the information for the necessary resolution within the domain would be represented. These points were chosen to be equally spaced along the jet sheet. The procedure may be outlined as follows; a more complete discussion of the numerical aspects of the method may be found in Ref. 13.

1) The iterative procedure was initiated with a set of values for the jet curvature $\kappa$. The curvature was employed as the primary representation of the jet rather than $f_J$ because it is of primary importance in the dynamical condition, and it is more sensitive variable than either $f_J$ or $df_J/dx$. The values of $\kappa$ were used to determine values for the jet slope at the control points $x_n$:

$$(df_J/dx)_{x_n} = \Lambda_n/(1-\Lambda_n^2)^{1/2} \tag{17}$$

where

$$\Lambda_n = \frac{-\tan(\tau+\alpha)}{[1+\tan^2(\tau+\alpha)]^{1/2}} + \int_0^{x_n} \kappa(x')\,dx' \tag{18}$$

An arbitrary set of values for $\kappa$, used to initiate each iteration, would not necessarily provide values for $\Lambda_n$ that would be properly bounded ($\Lambda_n < 1$). A multiplying factor for the set of values $\kappa$ was chosen to assure that condition.

2) With $df_J/dx$ known at each of the control points, a least-squares fit provided values for the coefficients ($a_i$) in the series approximation for $f_J$. This series provided a continuous functional form for $f_J$ and $df_J/dx$ within the near field.

3) The equidistant locations along the jet were obtained by numerically solving the first order, linear differential equation

$$d\xi/dx = [1 + (df_J/dx)^2]^{1/2} \tag{19}$$

where $\xi(0) = 0$.

4) The coefficients of the $C_n$ in Eqs. (11) and (12) then could be determined at each control point by numerical integration (compound Simpson's rule). Substituting Eqs. (11) and (12) into the dynamical condition, Eq. (15), one has a system of $N$ nonlinear algebraic equations for the $C_n$ values. The values of $C_n$ were obtained in a least-squares sense over the domain employing a secant method.

5) Given the set of $C_n$ values, a new set of values for $df_J/dx$, the slope of the jet sheet, was computed from Eq. (14). These values comprise a new description of the jet position. Since $\kappa$, rather than $df_J/dx$, was of principal interest, the

departures of $\kappa$ from the values employed to start the iteration were evaluated. Thus, if $\delta\kappa$ is the change in $\kappa$ predicted,

$$\delta\kappa = \frac{\delta(\mathrm{d}^2 f_J/\mathrm{d}x^2)}{[1+(\mathrm{d}f_J/\mathrm{d}x)^2]^{3/2}} - \frac{3(\mathrm{d}^2 f_J/\mathrm{d}x^2)(\mathrm{d}f_J/\mathrm{d}x)\delta(\mathrm{d}f_J/\mathrm{d}x)}{[1+(\mathrm{d}f_J/\mathrm{d}x)^2]^{5/2}} \tag{20}$$

Now, it was found that the first term of Eq. (20) could be neglected in the procedure (it could be expected to be small), and only the second was used. Convergence of the iteration procedure was speeded by choosing

$$\kappa_i^{n+1} = \kappa_i^n + e\,\delta\kappa_i \tag{21}$$

where the weighting factor $e$ was chosen initially to be small ($\sim 0.2$) and subsequently increased to 1 as the iterations progressed. With a new set of values for $\kappa_i$, the computation procedure would begin again at step 1 if the error criterion was not met.

A measure of the error in the results was obtained by comparing the new values of $\kappa_i$ with those employed upon starting the previous iteration. A sum of the squares of the relative errors $[\Sigma(\delta\kappa_i)^2]^{1/2}$ between these two values was employed in the computations for this purpose. If this sum was less than 0.6 (i.e., a 3% mean error at each control point), a solution was considered acceptable.

## Solution of the Airfoil Problem

There are two aspects of the aerodynamic field of the wing entering the theory. The first is the need for some initial estimate of the influence of the flowfield induced by the wing on the jet to start the computations. The second is the solution of the flowfield about the wing subject to the full influence of the disturbances introduced by the jet.

### Initial Estimate of the Flowfield of the Airfoil for Use in the Jet Problem

An initial estimate of the influence of the flowfield induced by the wing on the jet was obtained by means of a lifting line theory[14] for the computations reported herein. For an elliptically loaded wing operating with a lift coefficient $C_L$, the distribution of the vortex strength along the lifting line is given by

$$\Gamma = \Gamma_A[1+(y/s_A)^2]^{1/2} \tag{22}$$

where

$$\Gamma_A = \tfrac{1}{2} C_L U_\infty c(y=0)$$

The vorticity associated with the bound vortex line was placed on the quarter chord line of the wing and the trailing vorticity was regarded as lying in the $z=0$ plane. The value of $C_L$ employed was chosen to be higher than that for the wing alone, anticipating its enhancement by the jet flap. The induced velocity components were obtained from established relations presented in Ref. 15 and discussed in Ref. 13.

### Solution of the Flowfield about the Airfoil Subject to the Interference Field of the Jet

Given the solution of the jet problem, subject to the initial, estimated interaction of the wing, a more precise solution for the flowfield about the wing was obtained. This is formally given by the relation

$$V = U_\infty e_x + V_J + \frac{1}{4\pi}\iint_{S_A} \frac{\gamma_A' x R}{R^3}\,\mathrm{d}S' \tag{23}$$

subject to the kinematic condition [Eq. (2)]. It should be pointed out that, unlike most lifting surface theories, the streamwise disturbance velocity here is no longer negligible compared to the freestream velocity. The velocity field $V_J$ at points on the surface of the wing was obtained by integration over the known vortex strength distribution of the jet, from Eqs. (1).

Only wings with little or no dihedral (i.e., $\partial f_A/\partial y$ negligible) were considered in the computations. In addition, it was assumed that the spanwise velocity component was small compared to the downwash and the streamwise velocity components.

The surface over which the integral in Eq. (23) is evaluated includes the surface representing the wing (the projection of the wing onto the $z=0$ plane) *as well as a hypothetical surface containing the free vorticity washed downstream. It was simply assumed that the location of the free vorticity could be taken to lie in the* $z=0$ *plane.* This assumption is made in most wing theories and therefore allowed the utilization of some of the mathematical aspects of those theories. Written for a field point located on the wing, this integral results in an equation for the downwash velocity in terms of the difference in the pressure coefficients ($\Delta C_P$) across the wing

$$w_A(x,y,0) = -\frac{U_\infty^2}{8\pi} \fint_{-s_A}^{s_A} \frac{\mathrm{d}y'}{(y-y')^2} \int_{\text{l.e}}^{\text{t.e}} \frac{\Delta C_P}{(U_\infty + u_J)} \times\left(1+\frac{x-x'}{R}\right)\mathrm{d}x' \tag{24}$$

where $\fint$ denotes the Mangler principal value.[15]

Considering the wing to be composed of a number of finite, rectangular elements, in a manner similar to finite-element theories, the pressure difference across each element could be taken to be uniform. In addition, the velocity field induced by the jet was also assumed to be uniform over each element. The downwash (only due to the field of the wing) of the $k$th element at the $i$th control point may be written (cf., Fig. 2)

$$w_{A_{ki}} = -\frac{U_\infty^2 \Delta C_{Pk}}{8\pi(U_\infty + u_{Jk})} \int_{y_{ak}}^{y_{bk}} \frac{\mathrm{d}y'}{(y-y')^2} \int_{x_{ak}}^{x_{bk}} \left(1+\frac{x-x'}{R}\right)\mathrm{d}x' \tag{25}$$

The surface integral in Eq. (25) is only a function of the geometry of the element, and may be determined once and for all. The total downwash at a control point then could be determined by adding the contributions of the elements. The unknown pressure differences for the elements $\Delta C_{Pk}$ may be obtained by applying the kinematic condition at the $N$ control points, which were located at

$$x_i = x_{bi} + 0.1(x_{ai} - x_{bi})$$

$$y_i = 0.5(y_{ai} + y_{bi})$$

for the computations to be discussed in the next section. Once the pressure distribution on the airfoil was obtained, forces on the wing and the velocity field aft of the wing could be computed directly.

## Computational Results and Comparison with Experimental Data and Other Theories

Computed results were obtained for a rectangular wing with an aspect ratio ($AR$) of 6.8, equipped with a full span jet flap. Choice of the number of grid points employed to determine the necessary integrals and the number of control points on the wing and the jet was made on the basis of providing the highest accuracy for reasonable computational times on a CDC 6500 computer. By using 20 control points on the jet, and 32 elements on the wing, execution times of approximately 26 sec/iteration of the jet problem, and 23 sec to obtain the resulting forces on the wing and induced downwash at a downstream location were obtained. The near-field calculations were obtained in the region extending from the trailing edge of the airfoil to a point ($X$), approximately 10 chord lengths downstream. This region contained the major contributions to the vortex strength.

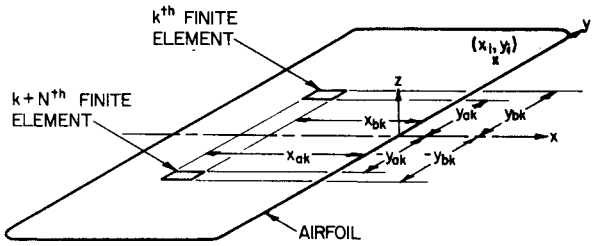


a) Location of the $k^{th}$ Finite Element and its Reflection

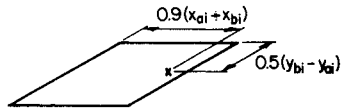


b) Location of the Control Point on the $i^{th}$ Element

**Fig. 2 Finite element geometry.**

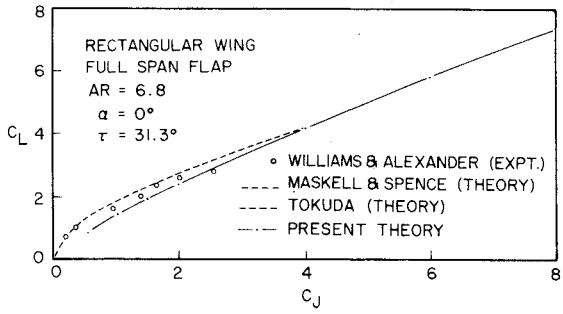


**Fig. 3 Variation of the lift coefficient with jet momentum flux for $\alpha = 0°$.**

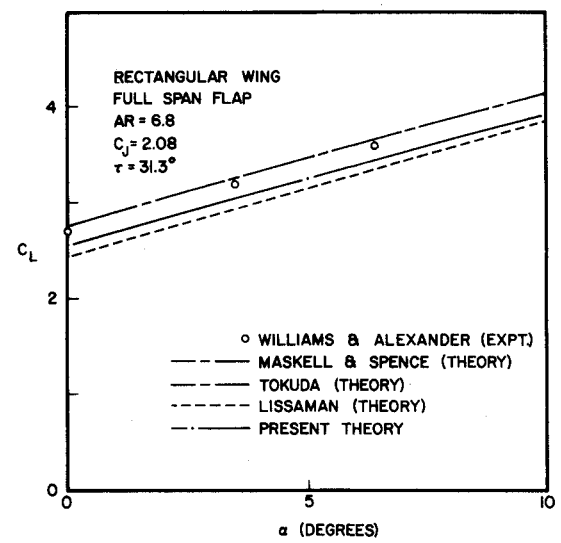


**Fig. 4 Variation of the lift coefficient with angle of attack for $C_J = 2.08$.**

Iterations of the entire problem were terminated once the relative error between two consecutive values of the lift coefficient was below 0.025. The preceding convergence criteria required approximately 3 iterations of the entire scheme, and an average of 6 iterations of the jet scheme. For the initial values, not close to the case considered, however, as many as 10 iterations were required to converge on a jet solution. As solutions were obtained for sets of values of $C_J$, $\alpha$, $\tau$, these were employed as initial conditions for successive

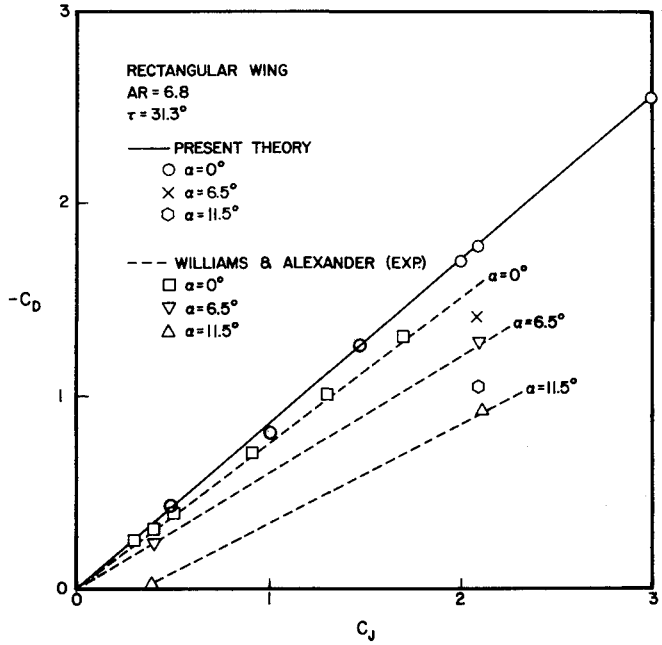


**Fig. 5 Drag coefficient as a function of jet momentum flux.**

solutions with slightly different values of the parameters, resulting in substantial time savings.

The variations of the lift coefficient with changes in the jet momentum coefficient are shown in Fig. 3. Comparison with the linear theories of Maskell and Spence[2] and Tokuda[4] are favorable. However, the values of $C_L$ computed by the present theory for large values of $C_J$ (nonlinear region) are evidently higher than what would be predicted by extending the curves obtained from the linear theories. Experimental data[15] also are available for the linear region. It can be seen in Fig. 3 that agreement between the present theory and the experimental data also are quite acceptable in that regime. It should be mentioned that the results of Maskell and Spence[2] accounted for the thickness of the wing employed in Williams'[15] experiments. Those of the present theory were not so adjusted. The thickness correction increases $C_L$. Within the region $0.5 < C_J < 4$, this factor has an average value of 1.08. Increasing the present theoretical results by this value yields even closer agreement with the experimental data.

The variation of $C_L$ with $\alpha$ is presented in Fig. 4. It can be seen in Fig. 4 that the variations of $C_L$ with changes in $\alpha$ from the present (nonlinear) theory lie slightly below the experimental data, which, in turn, are slightly below the curves obtained from the linear theories. It has been observed that linear theories, in general, tend to overestimate the lift, the difference increasing with larger values of $\alpha$ and $\tau$.[15] The linear theories represented in the curves employed a lifting-line approximation for the wing. It might be expected that the use of a lifting-surface technique would lower these values in a manner similar to that for conventional wings.[14] It has been suggested that the linear theories provide favorable agreement with the experimental data because of the "fortuitous cancellations" of higher order effects.[1] The results of Lissaman's theory[7,8] also are represented in Fig. 4. They tend to lie even lower than those of the present theory. The thickness correction employed by Maskell and Spence[2] would increase the values of the lift coefficient from the present theory by a factor of approximately 1.08. A corresponding increase in the results of the present theory would agree almost identically with the results of Williams.[15] The induced drag coefficients are presented in Fig. 5 as a function of $C_J$. The induced drag (or thrust for the conditions encountered) from the present theory only accounts for the reaction of the jet and the pressure distribution on the wing. Other contributions to the drag, form drag and viscous effects, such as skin friction or

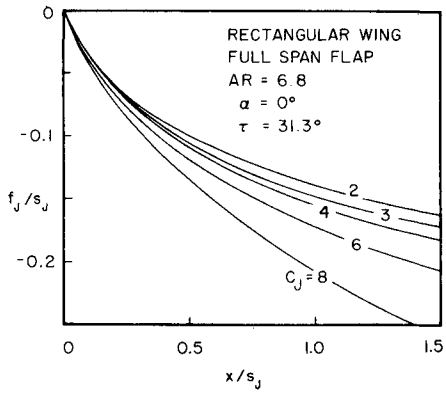


Fig. 6 Jet trajectories.

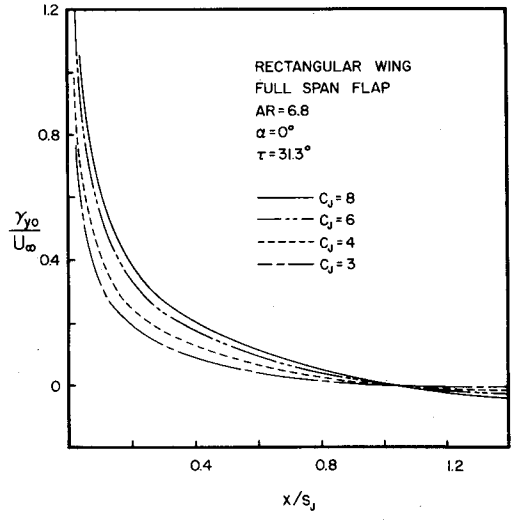


Fig. 7 Vortex strength in the plane of symmetry.

jet entrainment, are not represented in this analysis. It may be seen that the values obtained for the drag coefficient compare favorably with the data of Williams.[15]

Representative results for the jet sheet locations in the plane of symmetry are shown in Fig. 6 for different values of $C_J$. The jet lies well below the $z=0$ plane. Clearly for some conditions the positions of the jet sheet lie far from the plane of the wing suggesting the need for nonlinear theories such as that presented here, to describe the downwash near tail surfaces, etc. The vorticity distributions are illustrated in Fig. 7. It is apparent from this figure that the control points are located in a region ($x/s_J < 1.4$), which contains most of the vorticity. The distributions indicate that the vortex strength becomes slightly negative beyond $x=s_J$, a result of errors in the truncated series approximation employed for the vortex strength.

As a result of the large nose-down pitching moment experienced by an aircraft equipped with a jet flap, an exceptionally large amount of trim is required. Consequently, a control surface plays an important role in such configurations. It is important, therefore, to know the flowfield with some degree of accuracy in regions where the tail surface is to be located. Downwash results obtained from the present theory are shown in Fig. 8, in the form of the downwash angle ($\theta = \tan^{-1}(-U/W)$). The results were obtained at a representative point along the $x$ axis, three chord lengths downstream of the trailing edge of the wing. The large values of $\theta$ computed for the rather modest jet conditions illustrate the potential importance of the downwash in airframe design.

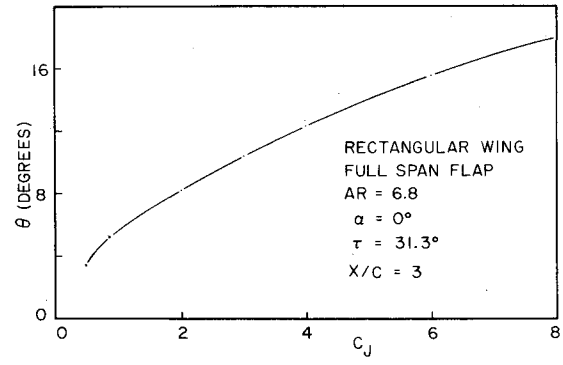


Fig. 8 Downwash angle for $\alpha = 0°$.

## Conclusions

The results of the present theory show ample agreement with the available data, and compare well with existing linear theories in the operating regime where they apply. For the lift coefficient, both the variation with $C_J$ and $\alpha$ found in the theory were satisfactory. The values of $C_L$ computed were slightly below the experimental data by an increment that could be accounted for easily by considering the wing thickness effect both in magnitude and trend. The induced drag (thrust) coefficient also agreed for the conditions considered. Regrettably, there are no experimental data available for the position of the jet sheet for a wing equipped with a jet flap for larger values of $C_J$, $\alpha$, or $\tau$. In addition, this theory extends values for the force system of the wing over a wide range of values for $C_J$ and $\tau$, beyond that for which the linear theories apply. Moreover, the downwash computations are likely to be a substantial improvement over results obtained from the linear theories.

In summary, the method developed here offers a fast, accurate procedure for analysis of jet flap-type configurations, including the domain of flight conditions where nonlinear effects may be important. The method may be extended easily to include entrainment effects,[16] more complete descriptions of aerodynamics of the wing, and ground effects. As experimental data become available for flows of this type, the model for the lateral vorticity distribution in the jet may be improved, but at the expense of simplicity in the mathematics.

## Acknowledgment

This work was sponsored by the NASA Langley Research Center, NASA Grant NGL 15-005-094.

## References

[1] Spence, D. A., "The Lift Coefficient of a Thin, Jet-Flapped Wing," *Proceedings of the Royal Society*, Vol. A238, Dec. 1956, pp. 46-68.

[2] Maskell, E. C., and Spence, D. A., "A Theory of the Jet Flap in Three Dimensions," *Proceedings of the Royal Society*, Vol. A251, June 1959, pp. 407-425.

[3] Kerney, K. P., "An Asymptotic Theory of the High-Aspect-Ratio Jet Flap," Ph.D. Thesis, School of Aeronautical Engineering, Cornell University, 1967.

[4] Tokuda, N., "An Asymptotic Theory of the Jet Flap in Three Dimensions," *Journal of Fluid Mechanics*, Vol. 46, Pt. 4, 1971, pp. 705-726.

[5] Lopez, M. L. and Shen, C. C., "Recent Developments in Jet Flap Theory and its Application to STOL Aerodynamics Analysis," AIAA Paper 71-578, June 1971.

[6] Shen, C. C., Lopez, M. L., and Wasson, N. F., "Jet Wing Lifting-Surface Theory Using Elementary Vortex Distributions," *Journal of Aircraft*, Vol. 12, May 1975, pp. 448-456.

[7] Lissaman, P. B. S., "A Linear Theory of the Jet Flap in Ground Effect," *AIAA Journal*, Vol. 6, July 1968, pp. 1356-1362.

[8] Lissaman, P. B. S., "Analysis of High-Aspect-Ratio Jet-Flapped Wings of Arbitrary Geometry," NASA CR-2179, 1973, pp. 1-56; also, *Journal of Aircraft*, Vol. 11, May 1974, pp. 259-265.

[9] Leamon, R. G. and Plotkin, A., "An Improved Solution of the Two-Dimensional Jet-Flapped Airfoil Problem," *Journal of Aircraft*, Vol. 9, Sept. 1972, pp. 631-635.

[10] Halsey, N. D., "Methods for the Design and Analysis of Jet-Flapped Airfoils," *Journal of Aircraft*, Vol. 11, Sept. 1974, pp. 540-546.

[11] Robinson, A. and Laurmann, J. A., *Wing Theory*, Cambridge University Press, Cambridge, 1956.

[12] Morse, P. M. and Feshbach, H., *Methods of Theoretical Physics*, McGraw-Hill, New York, 1953, Pt. I, pp. 52-54.

[13] Addessio, F. L. and Skifstad, J. G., "Theory of an Airfoil Equipped with a Jet Flap under Low-Speed Flight Conditions," NASA CR-2571, 1975.

[14] Thwaites, B., *Incompressible Aerodynamics*, Oxford University Press, Oxford, 1960.

[15] Williams, J. and Alexander, A. J., "Three-Dimensional Wind-Tunnel Tests of a 30° Jet Flap Model," Aeronautical Research Council C.P. No. 304, Nov. 1955.

[16] Wygnanski, I. and Newman, B. G., "The Effects of Jet Entrainment on Lift and Moment for a Thin Airfoil with Blowing," *Aeronautical Quarterly*, Vol. XV, Pt. 2, May 1964, pp. 122-150.